International Journal of Nanomedicine

Dovepress
open access to scientific and medical research

Open Access Full Text Article

ORIGINAL RESEARCH

Antimicrobial photodynamic activity and cytocompatibility of $Au_{25}(Capt)_{18}$ clusters photoexcited by blue LED light irradiation

This article was published in the following Dove Press journal:
International Journal of Nanomedicine
4 April 2017
Number of times this article has been viewed

Saori Miyata[1]
Hirofumi Miyaji[1]
Hideya Kawasaki[2]
Masaki Yamamoto[2]
Erika Nishida[1]
Hiroko Takita[3]
Tsukasa Akasaka[4]
Natsumi Ushijima[3]
Toshihiko Iwanaga[5]
Tsutomu Sugaya[1]

[1]Department of Periodontology and Endodontology, Hokkaido University Graduate School of Dental Medicine, Kita-ku, Sapporo, [2]Department of Chemistry and Materials Engineering, Faculty of Chemistry, Materials and Bioengineering, Kansai University, Suita-shi, Osaka, [3]Support Section for Education and Research, Hokkaido University Graduate School of Dental Medicine, [4]Department of Biomedical, Dental Materials and Engineering, Graduate School of Dental Medicine, Hokkaido University, [5]Department of Anatomy, Laboratory of Histology and Cytology, Hokkaido University Graduate School of Medicine, Kita-ku, Sapporo, Japan

Abstract: Antimicrobial photodynamic therapy (aPDT) has beneficial effects in dental treatment. We applied captopril-protected gold ($Au_{25}(Capt)_{18}$) clusters as a novel photosensitizer for aPDT. Photoexcited Au clusters under light irradiation generated singlet oxygen ($^1O_2$). Accordingly, the antimicrobial and cytotoxic effects of $Au_{25}(Capt)_{18}$ clusters under dental blue light-emitting diode (LED) irradiation were evaluated. $^1O_2$ generation of $Au_{25}(Capt)_{18}$ clusters under blue LED irradiation (420–460 nm) was detected by a methotrexate (MTX) probe. The antimicrobial effects of photoexcited Au clusters (0, 5, 50, and 500 μg/mL) on oral bacterial cells, such as *Streptococcus mutans, Aggregatibacter actinomycetemcomitans*, and *Porphyromonas gingivalis*, were assessed by morphological observations and bacterial growth experiments. Cytotoxicity testing of Au clusters and blue LED irradiation was then performed against NIH3T3 and MC3T3-E1 cells. In addition, the biological performance of Au clusters (500 μg/mL) was compared to an organic dye photosensitizer, methylene blue (MB; 10 and 100 μg/mL). We confirmed the $^1O_2$ generation ability of $Au_{25}(Capt)_{18}$ clusters through the fluorescence spectra of oxidized MTX. Successful application of photoexcited Au clusters to aPDT was demonstrated by dose-dependent decreases in the turbidity of oral bacterial cells. Morphological observation revealed that application of Au clusters stimulated destruction of bacterial cell walls and inhibited biofilm formation. Aggregation of Au clusters around bacterial cells was fluorescently observed. However, photoexcited Au clusters did not negatively affect the adhesion, spreading, and proliferation of mammalian cells, particularly at lower doses. In addition, application of Au clusters demonstrated significantly better cytocompatibility compared to MB. We found that a combination of $Au_{25}(Capt)_{18}$ clusters and blue LED irradiation exhibited good antimicrobial effects through $^1O_2$ generation and biosafe characteristics, which is desirable for aPDT in dentistry.

Keywords: *Aggregatibacter actinomycetemcomitans*, antimicrobial photodynamic therapy, photosensitizer, *Porphyromonas gingivalis*, singlet oxygen, *Streptococcus mutans*

Introduction

Antimicrobial photodynamic therapy (aPDT) is a reasonable strategy for light-mediated therapy. This therapy is based on an oxygen-dependent photochemical reaction that occurs upon light-mediated activation of a photosensitizing compound, leading to the generation of cytotoxic reactive oxygen species (ROS), including singlet oxygen ($^1O_2$) and superoxide.[1–3] ROS consistently exhibit antimicrobial and anticancer effects through severe damage to DNA and the cytoplasmic membrane.[3–5] It has been reported that aPDT rarely creates drug-resistant bacteria, which is an adverse effect of antibiotic therapy.[6] Since ROS exhibit a broad spectrum of antimicrobial activity, aPDT

Correspondence: Hirofumi Miyaji
Department of Periodontology and Endodontology, Hokkaido University Graduate School of Dental Medicine, N13 W7, Kita-ku, Sapporo 060-8586, Japan
Tel +81 11 706 4266
Fax +81 11 706 4334
Email miyaji@den.hokudai.ac.jp

submit your manuscript | www.dovepress.com
Dovepress
http://dx.doi.org/10.2147/IJN.S131602

causes damage to Gram-positive and -negative bacterial cells, fungi, and viruses. In addition, aPDT has the potential to destroy the biofilm matrix, in contrast to antibiotics.[1,7–10]

Recent developments in the field of dental aPDT have led to efficient dental treatments for caries, periodontitis, peri-implantitis, and endodontics.[6,11] To develop aPDT against these diseases, several organic dye photosensitizers, such as porphyrin,[12] rose Bengal,[13] indocyanine green,[14] toluidine blue,[15] and methylene blue (MB),[13] have been clinically used. However, these organic dyes have certain disadvantages in clinical use. For example, the ability to generate $^1O_2$ quickly disappears because of degradation of the photosensitizer.[16,17] Moreover, medical application of an organic photosensitizing agent commonly needs a cytotoxic organic solvent for formulation.[18] Therefore, the development of a biosafe photosensitizer is required for predictable clinical outcomes.

Recently, a captopril-protected gold cluster, consisting of 25 gold atoms and 18 captopril ligands as the protector, $Au_{25}(Capt)_{18}$, was developed as a novel photosensitizer not categorized as a conventional organic dye photosensitizer.[19] The $Au_{25}(Capt)_{18}$ cluster measures 0.9 nm in diameter; is highly stable, less degradable, and water-soluble; and produces $^1O_2$ on near-infrared light irradiation. Thus, $Au_{25}(Capt)_{18}$ clusters may resolve the problems associated with organic dye photosensitizers for aPDT. We speculated that Au clusters may possess new characteristics for dental aPDT compared with conventional photosensitizers. In addition to the near-infrared region, $Au_{25}(Capt)_{18}$ clusters have stronger absorbance in the range of 300–500 nm with a peak at 450 nm.[19] Thus, we anticipated that $Au_{25}(Capt)_{18}$ clusters photoexcited by a blue light-emitting diode (LED) light (ca. 450 nm) would be applicable for dental aPDT. The use of a light source for aPDT is attractive, since blue LED is commonly used as a dental curing device for polymerization of composite resin filling material in dental caries therapy. In addition, Chui et al[20] reported that blue light irradiation effectively inhibited the viability of bacterial cells. Thus, the combination of $Au_{25}(Capt)_{18}$ clusters and blue LED light is anticipated to exhibit synergistic antimicrobial effects. The local administration of Au clusters at the periodontal pocket or against root canal infection and subsequent LED irradiation may be a valuable antibacterial therapy in dentistry. However, application of Au clusters for dental aPDT has not been investigated thus far.

In this study, we report a new methodology for dental aPDT using $Au_{25}(Capt)_{18}$ clusters photoexcited by blue LED light. We evaluated whether $Au_{25}(Capt)_{18}$ clusters could produce $^1O_2$ on blue LED light irradiation and exert antibacterial activity against oral bacterial cells, *Streptococcus mutans, Aggregatibacter actinomycetemcomitans*, and *Porphyromonas gingivalis*. We also assessed the cytotoxicity of photoexcited Au clusters against fibroblastic NIH3T3 cells and osteoblastic MC3T3-E1 cells. Furthermore, cytotoxicity of Au clusters was compared to that of a conventional organic dye photosensitizer, MB, in dental aPDT.

Materials and methods

Synthesis of $Au_{25}(Capt)_{18}$ clusters

$Au_{25}(Capt)_{18}$ clusters were synthesized according to a previously described method.[19,21] Tetrachloroauric (III) acid (0.20 mmol, Wako Pure Chemical Industries Ltd., Osaka, Japan) and tetraoctylammonium bromide (0.23 mmol, Wako Pure Chemical Industries Ltd.) were dissolved in 10 mL methanol and stirred for 20 min. Subsequently, captopril (1 mmol, Tokyo Chemical Industry Co. Ltd., Tokyo, Japan) was dissolved in 5 mL methanol, injected in the reaction mixture, and further stirred for 30 min. Sodium borohydride (2 mmol) was dissolved in 5 mL of cold water and added to the mixture with stirring and kept under stirring for 8–12 h at room temperature. The resultant mixture was centrifuged to remove insoluble Au (I) polymer. The supernatant was collected and concentrated by rotary evaporation and then $Au_{25}(Capt)_{18}$ clusters were precipitated by ethanol and dried in a vacuum. The generation of $Au_{25}(Capt)_{18}$ clusters was confirmed by a ultraviolet-visible (UV-vis) spectrophotometer (V-670 UV-VIS-NIR Spectrophotometer, Jasco, Tokyo, Japan) and a spectrofluorometer (FP-6300 Spectrometer, Jasco).

Detection of $^1O_2$ generation by $Au_{25}(Capt)_{18}$ clusters

$^1O_2$ generation by photoexcited $Au_{25}(Capt)_{18}$ clusters under blue LED light irradiation was evaluated using methotrexate (MTX, Wako Pure Chemical Industries Ltd.) as a chemical probe of $^1O_2$. MTX can selectively react with $^1O_2$, resulting in an increased fluorescence intensity.[22] The concentration of the Au clusters was adjusted to be equal absorbance (ca. 0.1) at 532 nm. A 10-mM stock solution of MTX in *N,N*-dimethylformamide was prepared and then added to a 2-mL aqueous solution (D_2O) to yield a final concentration of MTX of 20 μM. The solutions were then irradiated with a blue LED light device at a wavelength of 420–460 nm (1 W/cm^2, PenCure, Morita Corporation, Tokyo, Japan). The fluorescence spectra were recorded using a spectrofluorometer (FP-6300, Jasco).

Preparation of bacterial suspension

Facultative anaerobic bacteria, *S. mutans* ATCC 35668 and *A. actinomycetemcomitans* ATCC 29522, and obligate

anaerobic bacteria, *P. gingivalis* ATCC 33277, were kept frozen until analysis. The stocks were incubated in brain heart infusion (BHI) broth (Pearlcore®, Eiken Chemical Co. Ltd., Tokyo, Japan) supplemented with 0.1% antibiotic (gramicidin D and bacitracin, Wako Pure Chemical Industries Ltd.) and 1% sucrose for *S. mutans*; 1% yeast extract (Wako Pure Chemical Industries Ltd.) for *A. actinomycetemcomitans*; and 0.5% yeast extract, 0.0005% hemin, and 0.0001% menadione for *P. gingivalis*.

Antimicrobial effects of $Au_{25}(Capt)_{18}$ clusters and blue LED on *S. mutans*

According to the report by Kawasaki et al,[19] the upper limit of Au clusters that did not affect the survival of HeLa cells was 500 μg/mL. Therefore, we selected 500 μg/mL as the maximum concentration of Au clusters. $Au_{25}(Capt)_{18}$ clusters (final concentration: 0, 5, 50, and 500 μg/mL) were dissolved in the suspension of *S. mutans* (final concentration: 5.5×10^6 colony-forming unit [CFU]/mL) and dispensed into microplates. This suspension was irradiated by blue LED light for 1 min before incubation. Medium exchange and subsequent blue LED irradiation for 1 min were performed every 24 h under anaerobic incubation at 37°C. As a control, a suspension without LED irradiation was assessed.

For morphological observations of *S. mutans* after incubation for 4, 24, or 72 h, inoculated samples were fixed in 2.5% glutaraldehyde in 0.1 M sodium cacodylate buffer (pH 7.4) and then dehydrated in increasing concentrations of ethanol. After critical point drying and Pt-PD coating, the samples were analyzed using scanning electron microscopy (SEM; S-4000, Hitachi Ltd., Tokyo, Japan) at an accelerating voltage of 10 kV. Fixed samples after 48-h incubation were postfixed in 1% OsO_4 and 0.1 M sodium cacodylate buffer (pH 7.4) at 4°C for 1 h. Using the standard procedure, samples were dehydrated in ethanol, infiltrated with propylene oxide, and embedded in Epon. The samples were sliced and characterized using transmission electron microscopy (TEM; HD-2000, Hitachi Ltd.) at 200 kV acceleration voltage.

S. mutans samples incubated for 24 h were stained by the LIVE/DEAD BacLight Bacterial Viability Kit (Thermo Fisher Scientific, Waltham, MA, USA), according to the manufacturer's instructions. Live bacteria were stained with SYTO 9 to produce green fluorescence and bacteria with compromised membranes were stained with propidium iodide to produce red fluorescence. Samples were observed using confocal laser scanning microscopy (FluoView, Olympus Corporation, Tokyo, Japan).

To confirm the locations of Au clusters after application to bacterial suspension, carboxylic acid of $Au_{25}(Capt)_{18}$ clusters was labeled with a reactive dye (Alexa Fluor 488 Hydroxylamine, Thermo Fisher Scientific). Two hundred microliters of 1 mg/mL dye and 2 mL of 1 mg/mL Au clusters were mixed and stirred for 15 min. The mixture and *S. mutans* suspension (1:1) were placed on a glass-bottomed dish and observed by fluorescence laser scanning microscopy (Biorezo BZ-9000, Keyence Corporation, Osaka, Japan). As a control, a mixture of bacterial suspension and reactive dye (no Au clusters) was assayed in the same manner.

After incubation for 24 h, the turbidity of each suspension was measured using a turbidimeter (CO7500 Colourwave, Funakoshi Co. Ltd., Tokyo, Japan) at 590 nm. Some samples were used to assess CFU. *S. mutans* suspensions including $Au_{25}(Capt)_{18}$ clusters (500 μg/mL) were diluted 10-fold in fresh BHI broth and spread onto BHI agar plates (Eiken Chemical Co. Ltd.). After incubation at 37°C for 48 h, *S. mutans* CFUs were determined. In addition, to examine the effect of light irradiation frequency, light irradiation of various exposure times, 30, 60, and 90 s, was applied to *S. mutans* suspensions including Au clusters (500 μg/mL), and then the bacterial turbidity was measured. The viability and lactate acid productivity of *S. mutans* were assessed using water-soluble tetrazolium salt (WST)-8 (Cell Counting Kit-8, Dojindo Laboratories, Mashiki, Japan) and lactate assay kit II (BioVision Inc., Milpitas, CA, USA), respectively, according to the manufacturers' instructions. The absorbance was measured using a microplate reader (ETY-300, Toyo Sokki, Yokohama, Japan) at 450 nm.

Turbidity assays of *A. actinomycetemcomitans* and *P. gingivalis*

$Au_{25}(Capt)_{18}$ clusters (final concentration: 0, 5, 50, and 500 μg/mL) were dispersed in suspensions of *A. actinomycetemcomitans* (final concentration: 1×10^5 CFU/mL) and *P. gingivalis* (final concentration: 1.6×10^7 CFU/mL) and dispensed into 96-well plates. Before incubation, the suspension was irradiated with blue LED light for 1 min. As a control, suspensions with no LED irradiation were measured. After incubation at 37°C under anaerobic conditions for 24 h, the bacterial turbidity was measured using a turbidimeter.

Cytotoxic assessment of $Au_{25}(Capt)_{18}$ clusters and blue LED

To evaluate cytotoxicity, 1×10^4 mouse osteoblastic MC3T3-E1 cells (RIKEN BioResource Center, Tsukuba, Japan) and fibroblastic NIH3T3 cells (RIKEN BioResource Center) were grown in 96-well plates using culture medium

(minimum essential medium alpha, GlutaMAX-I, Thermo Fisher Scientific) supplemented with 10% fetal bovine serum (Qualified FBS, Thermo Fisher Scientific) and 1% antibiotics (Penicillin-Streptomycin, Thermo Fisher Scientific). $Au_{25}(Capt)_{18}$ clusters were added into the medium at final concentrations of 0, 5, 50, and 500 μg/mL. Before incubation, suspensions were irradiated with blue LED light for 1 min. The cultures were incubated at 37°C with 5% CO_2. Medium exchange and subsequent blue LED irradiation for 1 min were performed every 2 days. As a control, nonirradiated suspensions were assessed. The cytotoxicity after incubation for 2, 4, and 6 days was determined using the WST-8 assay (Dojindo Laboratories) and lactate dehydrogenase (LDH) assay (Cytotoxicity LDH Assay Kit-WST, Dojindo Laboratories) following the manufacturer's instructions. The absorbance at 450 nm (WST-8) and 490 nm (LDH) was measured on a microplate reader.

Some samples incubated for 24 h were morphologically analyzed using SEM. In addition, fluorescence observation through vinculin-F-actin double staining was performed. The cultured cells were washed with phosphate-buffered saline (PBS) and fixed with 3.5% formaldehyde in PBS for 5 min. After fixation and washing with PBS, cells were permeabilized with 0.5% Triton X-100 for 10 min and washed again with PBS. Then, cells were incubated for 30 min with bovine serum albumin (7.5 w/v% Albumin Dulbecco's PBS (−) Solution, from Bovine Serum, Wako Pure Chemical Industries Ltd.) as blocking buffer and washed with PBS. Four microliters of 0.5 mg/mL anti-vinculin monoclonal antibody (Anti-Vinculin Alexa Fluor 488, eBioscience, San Diego, CA, USA) and 3 μL of 20 μg/mL phalloidin (Acti-stain 555 fluorescent Phalloidin, Cytoskeleton Inc., Denver, CO, USA) were diluted in 500 μL of methanol, 3 μL of 1 mg/mL 4′, 6-diamidino-2-phenylindole solution (Dojindo Laboratories), and 500 μL of bovine serum albumin, and the mixture was kept shaking for 1 h at 37°C. After standing for 1 day at 4°C, the sample was washed three times with PBS (except for liquids) and then covered with a cover glass. The cells were observed using fluorescence laser scanning microscopy.

Some samples were stained using the LIVE/DEAD Viability/Cytotoxicity Kit for mammalian cells (Thermo Fisher Scientific), following the manufacturer's instructions. Stained samples were examined using confocal laser scanning microscopy.

Comparative cytotoxic evaluation of $Au_{25}(Capt)_{18}$ clusters and MB

We prepared aqueous solutions of $Au_{25}(Capt)_{18}$ clusters (500 μg/mL) and MB (10 and 100 μg/mL, Wako Pure Chemical Industries Ltd.) for comparative cytotoxic examinations without LED irradiation. In this experiment, MB concentrations were selected according to previous reports of aPDT using MB.[23,24] Photosensitizers were dispersed in suspensions containing *A. actinomycetemcomitans* and *P. gingivalis*. After 24-h incubation, the optical density was measured for bacterial turbidity using a turbidimeter.

Cytotoxicity assessments of $Au_{25}(Capt)_{18}$ clusters or MB solutions were carried out using osteoblastic MC3T3-E1 and fibroblastic NIH3T3 cells. The cultures were grown in 96-well plates and incubated at 37°C with 5% CO_2. After culturing for 2, 4, and 6 days, the cytotoxicity was determined using WST-8 and LDH assays. In addition, SEM observation and fluorescence staining were performed for samples receiving $Au_{25}(Capt)_{18}$ clusters or MB.

Statistical analysis

Statistical analysis was performed by Scheffe's test. *P*-values <0.05 were considered statistically significant. All statistical procedures were performed using a software package (Statistical Package for the Social Sciences [SPSS] 11.0, IBM Corporation, Armonk, NY, USA).

Results

Synthesis of $Au_{25}(Capt)_{18}$ clusters

The prepared $Au_{25}(Capt)_{18}$ clusters were water-soluble and the aqueous solution of $Au_{25}(Capt)_{18}$ clusters exhibited a brown color (Figure 1A). The generation of $Au_{25}(Capt)_{18}$ clusters was confirmed by the UV-vis spectrum, showing two main absorption bands at 450 and 670 nm, and a broad shoulder at ca. 800 nm (Figure 1B), which was consistent with those in previous reports on $Au_{25}(Capt)_{18}$ clusters.[19,21]

Detection of $^1O_2$ generation by $Au_{25}(Capt)_{18}$ clusters

In the present study, an MTX probe was employed to examine the $^1O_2$ generation ability of $Au_{25}(Capt)_{18}$ clusters. It has been reported that $^1O_2$ can selectively react with MTX to form an oxidation product, resulting in increased fluorescence intensity.[18] The fluorescence spectra of MTX in the presence of the $Au_{25}(Capt)_{18}$ clusters in D_2O were determined. In control (no application of $Au_{25}(Capt)_{18}$ clusters), there was no change in the fluorescence spectra of MTX after blue LED light irradiation to only MTX for 1 min. This indicates that MTX was not oxidized by $^1O_2$ under only blue LED light irradiation. In the presence of $Au_{25}(Capt)_{18}$ clusters, the fluorescence intensities of MTX at 466 nm increased

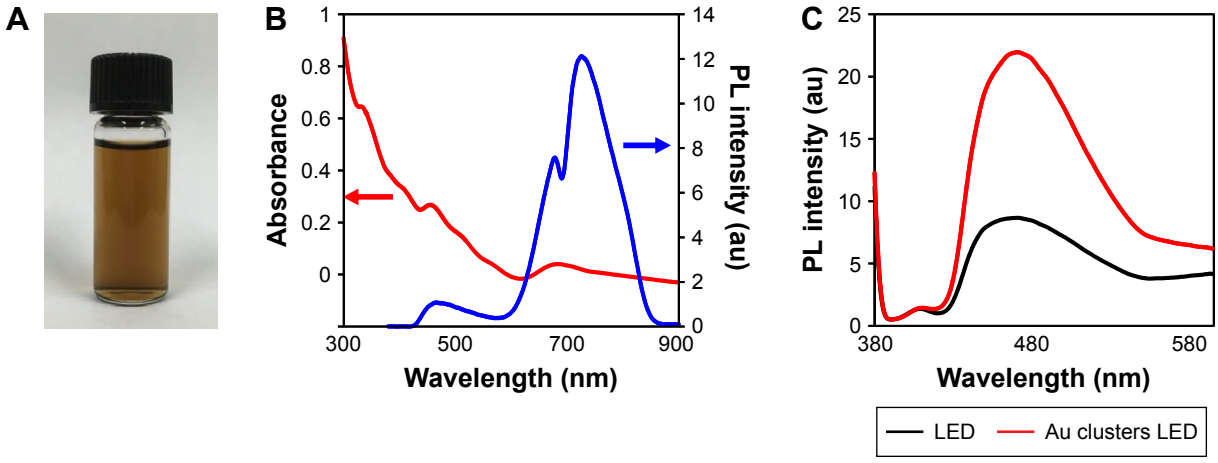

Figure 1 Optical properties of $Au_{25}(Capt)_{18}$ clusters.
Notes: (**A**) Aqueous solution of dispersed $Au_{25}(Capt)_{18}$ clusters. (**B**) The ultraviolet–visible wavelength spectrum (red line) and fluorescence spectrum (blue line) of $Au_{25}(Capt)_{18}$ clusters. (**C**) Fluorescence spectra of a methotrexate-containing solution of $Au_{25}(Capt)_{18}$ clusters.
Abbreviations: LED, light-emitting diode; PL, photoluminescence.

because of the oxidation of MTX with $^1O_2$ generated by photoexcited $Au_{25}(Capt)_{18}$ clusters (Figure 1C). The result indicates that $Au_{25}(Capt)_{18}$ clusters generated $^1O_2$ with blue LED irradiation.

Morphological analysis of *S. mutans* receiving $Au_{25}(Capt)_{18}$ clusters and blue LED

The SEM images of *S. mutans* at 4, 24, and 72 h after incubation are shown in Figure 2A–L. In control (no application of Au clusters and no light irradiation), marked colonization of *S. mutans* was observed on the culture dish at 24 h, and a thick biofilm was detected at 72 h (Figure 2A, E, and I). Samples exposed to blue LED light alone produced a biofilm microscopically resembling control samples (Figure 2B, F, and J). In contrast, the sample groups including $Au_{25}(Capt)_{18}$ clusters showed slight bacterial accumulation and biofilm formation throughout the examination period (Figure 2C, D, G, H, K, and L). TEM observation (Figure 3A–D) revealed that the cell wall of *S. mutans* cells was destroyed, and ultrafine particles (shown by arrows in Figure 3C and D) were frequently observed in and around *S. mutans* cells in the presence of $Au_{25}(Capt)_{18}$ clusters. In LIVE/DEAD BacLight staining of *S. mutans* (Figure 3E–H), we confirmed that *S. mutans* stained red, indicating dead cells, and the number of red cells increased in the presence of $Au_{25}(Capt)_{18}$ clusters under irradiation with blue LED light. The combined application of Au clusters and irradiation resulted in a significant increase in red fluorescence emissions from dead cells (Figure 3H). In addition, aggregates of Alexa Fluor 488-labeled Au clusters were fluorescently detected corresponding to the location of *S. mutans* cells on dishes (Figure 3I and J). Samples without *S. mutans* revealed no detectable signal (data not shown).

Antimicrobial effects of $Au_{25}(Capt)_{18}$ clusters and blue LED on oral bacterial cells

Figure 4A and B shows the turbidity and viability of *S. mutans*, respectively. Application of $Au_{25}(Capt)_{18}$ clusters reduced bacterial turbidity and viability in a dose-dependent manner. In particular, blue LED light irradiation in the presence of 500 μg/mL $Au_{25}(Capt)_{18}$ clusters significantly decreased turbidity and viability of *S. mutans* in all samples. Similarly, CFUs of *S. mutans* incubated with Au clusters (500 μg/mL) were lower than those of control samples. In particular, photoexcited Au clusters reduced *S. mutans* concentration (CFU/mL) by three orders of magnitude compared to control (Figure S1). The turbidity of *S. mutans* with Au clusters application decreased after long-term light irradiation (Figure 4C), and the turbidity of samples after 60- and 90-s irradiation was lower than that of control (no Au clusters application). The result of the lactate acid assay is shown in Figure 4D. Combined application of 500 μg/mL $Au_{25}(Capt)_{18}$ clusters and blue LED irradiation strongly reduced the acid production by *S. mutans* compared with those of other groups.

To examine the antimicrobial activity of $Au_{25}(Capt)_{18}$ clusters on periodontal bacteria, we also examined the turbidity of *A. actinomycetemcomitans* and *P. gingivalis*, which are well-established periodontal bacteria, in the presence of $Au_{25}(Capt)_{18}$ clusters (Figure 4E and F). Interestingly, addition of $Au_{25}(Capt)_{18}$ clusters consistently lowered the turbidity

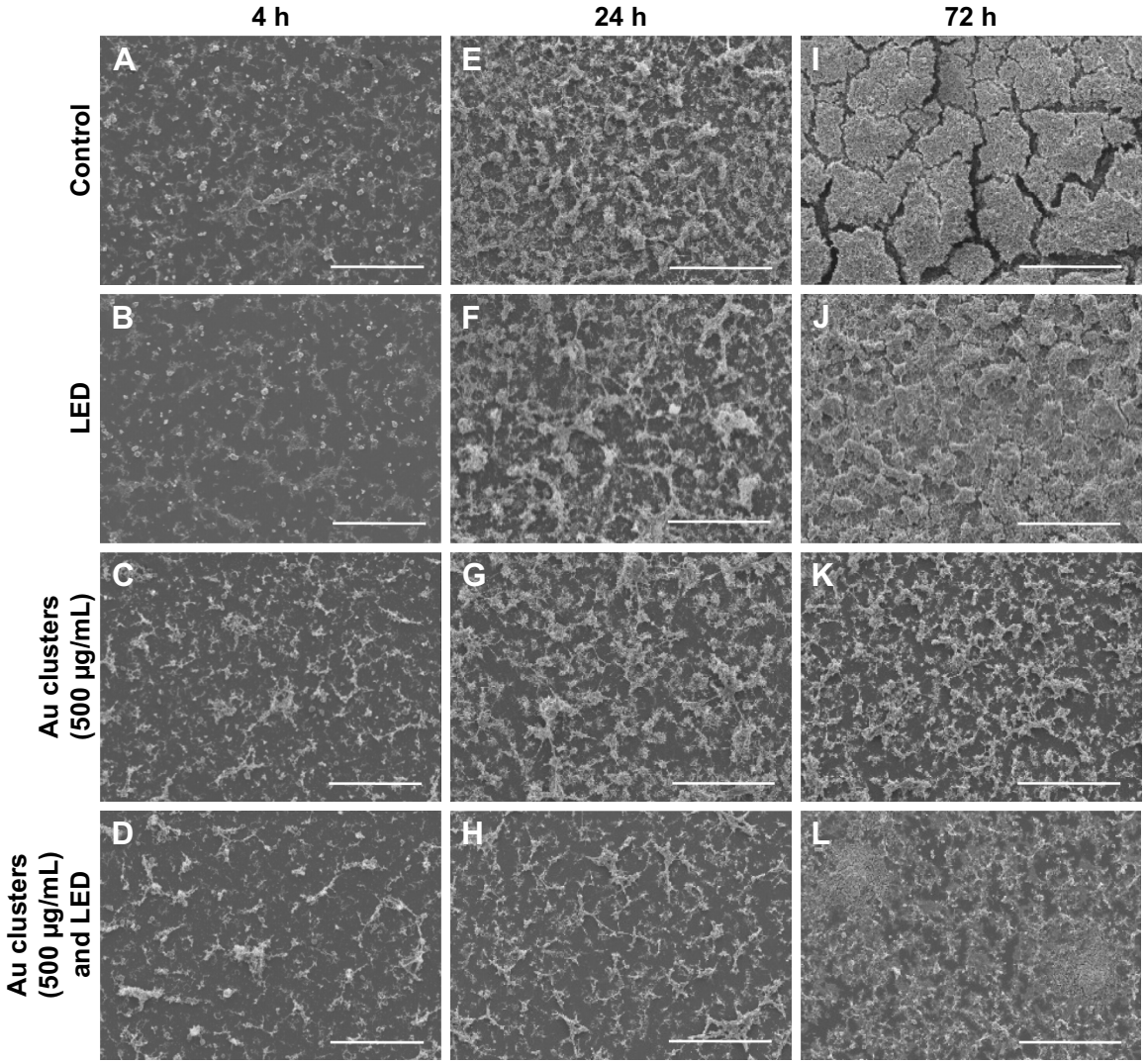

Figure 2 SEM observation of *Streptococcus mutans*.
Notes: (**A**–**L**) SEM micrographs of *S. mutans* after incubation for 4 h (**A**–**D**), 24 h (**E**–**H**), and 72 h (**I**–**L**). Application of Au clusters and LED irradiation decreased bacterial accumulation and biofilm formation compared to control (no application of Au clusters and no light irradiation) and LED light alone. Scale bar represents 100 µm (**A**–**L**).
Abbreviations: LED, light-emitting diode; SEM, scanning electron microscopy.

of bacterial suspensions, regardless of application of blue LED irradiation, in contrast to the assessment of *S. mutans*. The combination of $Au_{25}(Capt)_{18}$ clusters and LED irradiation significantly reduced the turbidity of *A. actinomycetemcomitans* and *P. gingivalis*, especially at 50 and 500 µg/mL $Au_{25}(Capt)_{18}$ clusters, compared with other groups.

Cytotoxic effect of $Au_{25}(Capt)_{18}$ clusters and blue LED light

To examine the cytotoxicity of $Au_{25}(Capt)_{18}$ clusters and blue LED light irradiation, SEM observation, vinculin-F-actin double staining, and LIVE/DEAD staining were performed for NIH3T3 and MC3T3-E1 cells. The morphology of incubated NIH3T3 and MC3T3-E1 cells was equivalent between examination and control groups in SEM observation (Figure 5A–D). Vinculin and F-actin were expressed as cell attachment and spreading with fine process elongation and pseudopods were detected regardless of application of $Au_{25}(Capt)_{18}$ clusters and blue LED irradiation (Figure 5E–H). In addition, the LIVE/DEAD BacLight assay showed that all samples consistently exhibited green fluorescence (live cells; Figure 5I–L).

The results of WST-8 and LDH assays are presented in Figure 6. At 2 days, cells were equivalently proliferated regardless of the application of $Au_{25}(Capt)_{18}$ clusters under blue LED irradiation. However, at 4 and 6 days for NIH3T3 cells and at 6 days for MC3T3-E1 cells, cell proliferation was significantly decreased by application of $Au_{25}(Capt)_{18}$ clusters in a dose-dependent manner. In particular, the combination of Au clusters and blue LED irradiation suppressed cell

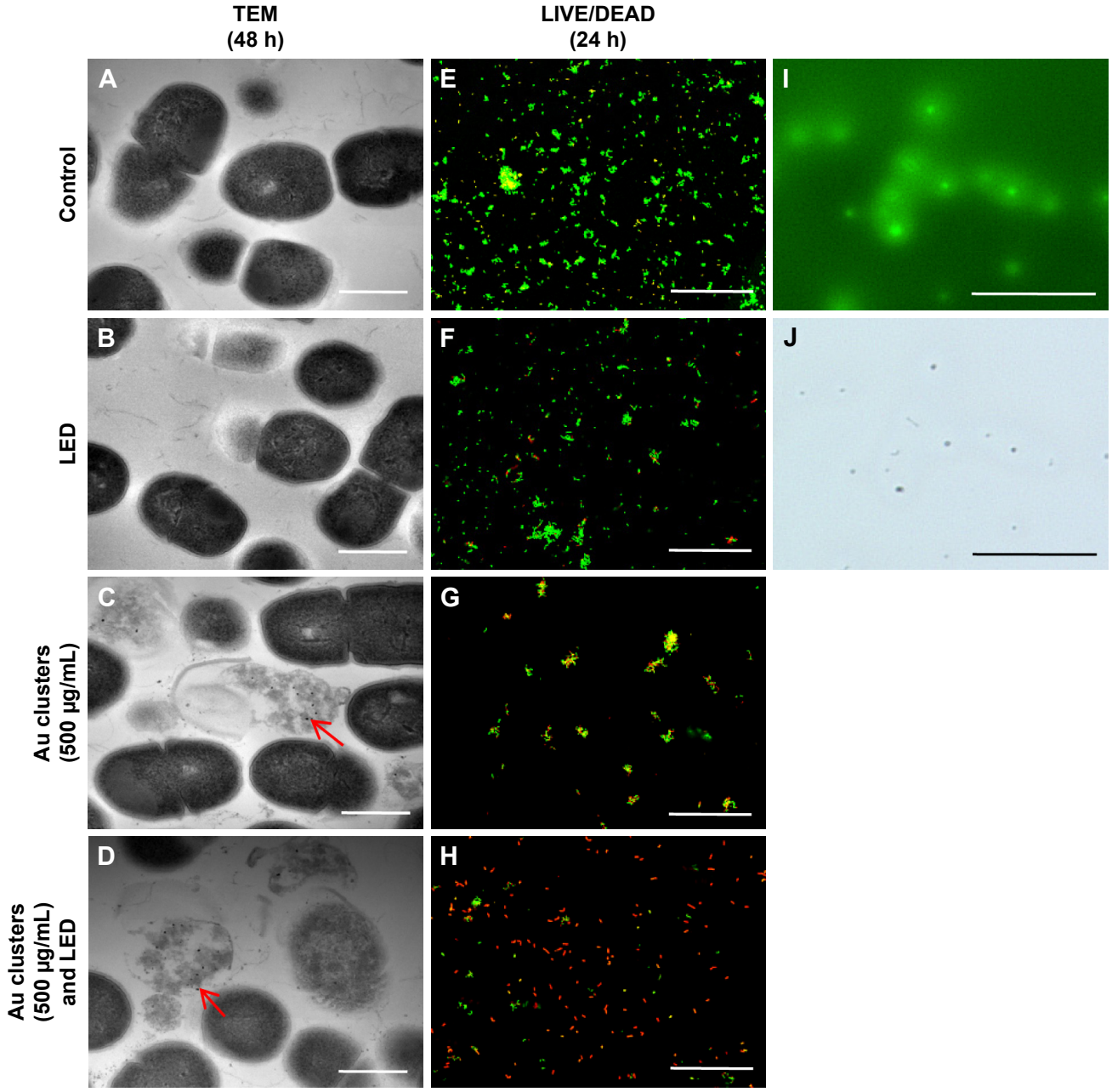

Figure 3 Morphological and fluorescence examinations of *Streptococcus mutans*.
Notes: (**A**–**D**) TEM micrographs of *S. mutans* after 48 h incubation. Arrows indicate ultrafine particles. (**E**–**H**) LIVE/DEAD BacLight staining of *S. mutans* after 24-h incubation. (**I**, **J**) Fluorescence examination of labeled Au clusters (500 μg/mL). Fluorescence image (**I**) and light field image (**J**). Scale bar represents 1 μm (**A**–**D**) and 50 μm (**E**–**J**).
Abbreviations: LED, light-emitting diode; TEM, transmission electron microscopy.

viability. The LDH assay showed that 50 and 500 μg/mL $Au_{25}(Capt)_{18}$ clusters enhanced LDH activity 2 days after incubation. In contrast, low-dose $Au_{25}(Capt)_{18}$ clusters (5 μg/mL) led to low LDH activity and no significant difference compared to control.

Comparative cytotoxic evaluations of $Au_{25}(Capt)_{18}$ clusters and MB

SEM and fluorescence microscope images of NIH3T3 and MC3T3E1 cells receiving photosensitizers (under non-LED irradiation condition) are shown in Figure 7A–L. Following application of 10 and 100 μg/mL MB, cell spreading, including the development of stress fibers and vinculin expression, was significantly inhibited compared with 500 μg/mL $Au_{25}(Capt)_{18}$ clusters receiving group. In particular, the addition of 100 μg/mL MB resulted in ball-shaped cells (Figure 7C, F, I, and L). The result of the WST-8 assay is shown in Figure 8A and B. Application of $Au_{25}(Capt)_{18}$ clusters consistently stimulated cell proliferation compared to MB. Marked suppression of cell viability was observed with application of 100 μg/mL MB.

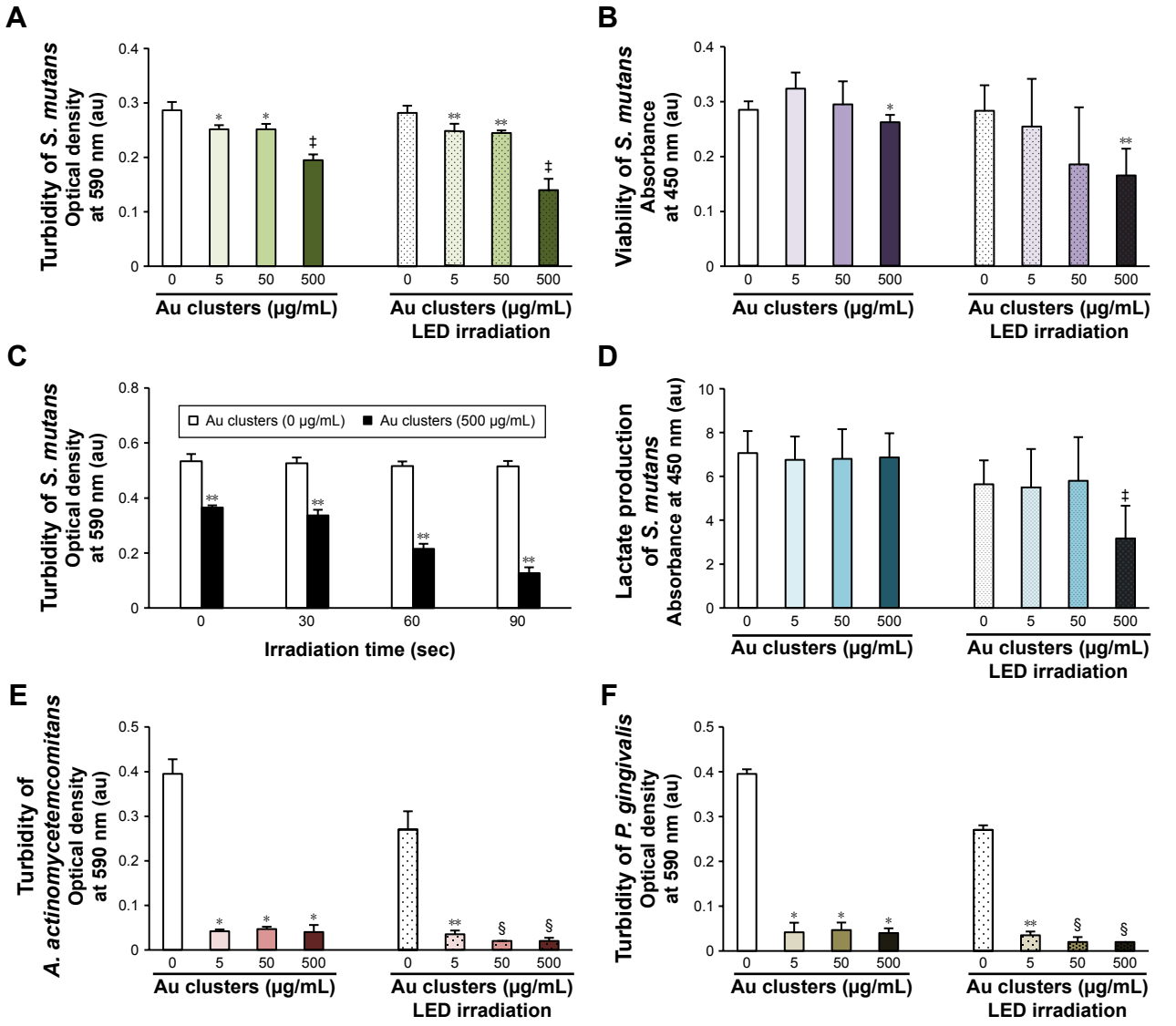

Figure 4 Antimicrobial effects of Au clusters on oral bacterial cells after 24-h incubation (n=6, mean ± standard deviation).
Notes: (**A**) Turbidity of *S. mutans*. (**B**) Viability of *S. mutans*. (**C**) Turbidity of *S. mutans* related to irradiation time. (**D**) Lactate production of *S. mutans*. (**E**) Turbidity of *A. actinomycetemcomitans*. (**F**) Turbidity of *P. gingivalis*: **P*<0.05 vs 0 μg/mL Au clusters; ***P*<0.05 vs 0 μg/mL Au clusters after LED irradiation; ‡*P*<0.05 vs all other groups; and §*P*<0.05 vs 0 and 5 μg/mL Au clusters after LED irradiation.
Abbreviations: au, arbitrary unit; LED, light-emitting diode; *A. actinomycetemcomitans*, *Aggregatibacter actinomycetemcomitans*; *P. gingivalis*, *Porphyromona gingivalis*; *S. mutans*, *Streptococcus mutans*.

The turbidity of *A. actinomycetemcomitans* and *P. gingivalis* was strongly decreased upon application of 500 μg/mL $Au_{25}(Capt)_{18}$ clusters or 10 and 100 μg/mL MB (Figure 8C, D). Overall, 100 μg/mL MB exhibited the greatest antimicrobial effect, although MB had higher cytotoxicity than $Au_{25}(Capt)_{18}$ clusters. The turbidity of samples receiving 500 μg/mL $Au_{25}(Capt)_{18}$ clusters was not significantly different than those receiving 10 μg/mL MB.

Discussion

In this study, we confirmed the generation of $^1O_2$ from $Au_{25}(Capt)_{18}$ clusters photoexcited by blue LED light. $^1O_2$ can be produced by photosensitizers related to the type II pathway, that is, energy transfer during a collision between the excited photosensitizer and $^3O_2$.[1,2] The predominant antimicrobial effect of $^1O_2$ is by oxidation of biological molecules. Oxidative stress mediated by ROS can attack polyunsaturated fatty acids in membranes and stimulate lipid peroxidation to impair membrane functions and produce toxic products, such as aldehydes.[25] The secondary production and storage of aldehydes cause damage of biological molecules.[26] In addition, ROS destroy the ligation moieties of nucleic acids, base and sugar groups, and subsequently suspend DNA replication.[27] Furthermore, generation of ROS leads to the modification of amino acid side chains of proteins, causing degradation. Damaged proteins subsequently affect

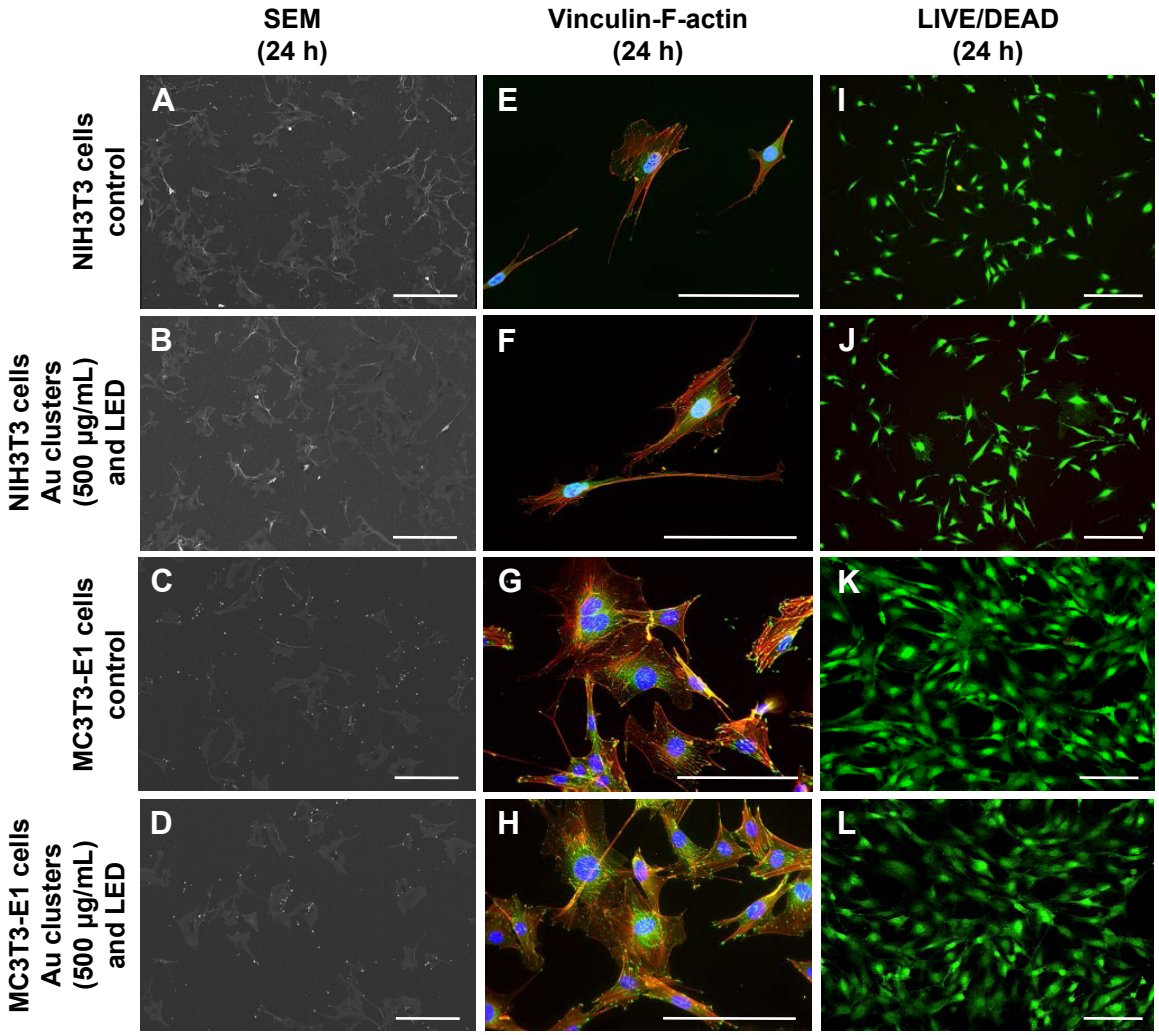

Figure 5 Evaluation of cell morphology after 24-h incubation.
Notes: (**A**–**D**) SEM observation. (**E**–**H**) Vinculin-F-actin double staining. (**I**–**L**) LIVE/DEAD BacLight staining. The morphology of NIH3T3 and MC3T3-E1 cells following application of Au clusters and LED irradiation was similar to that of control (no application of Au clusters and no light irradiation). Scale bar represents 200 μm (**A**–**D**), 50 μm (**E**–**H**), and 100 μm (**I**–**L**).
Abbreviations: LED, light-emitting diode; SEM, scanning electron microscopy.

intracellular pathways and disturb cellular metabolism.[27] Ichinose-tsuno et al[28] reported that aPDT using toluidine blue O and red LED facilitated an inhibitory effect on plaque formation. Fontana et al[29] and O'Neill et al[30] showed that application of dye photosensitizers, including MB and toluidine blue O, under red light irradiation inhibited plaque formation and significantly increased bacterial cell death and destruction of biofilms in the oral cavity, suggesting that $^1O_2$ could penetrate dental plaque and subsequently cause destruction through antimicrobial effects. From these results, $^1O_2$ produced by $Au_{25}(Capt)_{18}$ clusters under blue LED light likely plays a major role in the antimicrobial effect on oral flora observed in this study.

Antimicrobial assessments revealed that the turbidity and viability of *S. mutans* were gradually reduced by application of $Au_{25}(Capt)_{18}$ clusters under blue LED light in a cluster dose- and irradiation time-dependent manner. On SEM observation, bacterial colonies were fewer in the photoexcited $Au_{25}(Capt)_{18}$ clusters receiving group compared to control. It is likely that $^1O_2$ generated by photoexcited $Au_{25}(Capt)_{18}$ clusters suppressed *S. mutans* growth and bacterial aggregate formation. LIVE/DEAD BacLight staining observation revealed that dead bacteria were significantly observed in samples that received photoexcited $Au_{25}(Capt)_{18}$ clusters. In addition, we frequently found *S. mutans* cells with irregular cell walls in TEM images (Figure 3), suggesting that the bacteria cell wall was destroyed by $^1O_2$, consequently inducing cell death. In general, as $^1O_2$ quickly disappears in ca. 3.5 μs following its generation,[20] the distance of $^1O_2$ diffusion to the bacterial cells is a very important factor of aPDT activity. The TEM image of the $Au_{25}(Capt)_{18}$ clusters receiving group showed that many ultrafine dots were present in

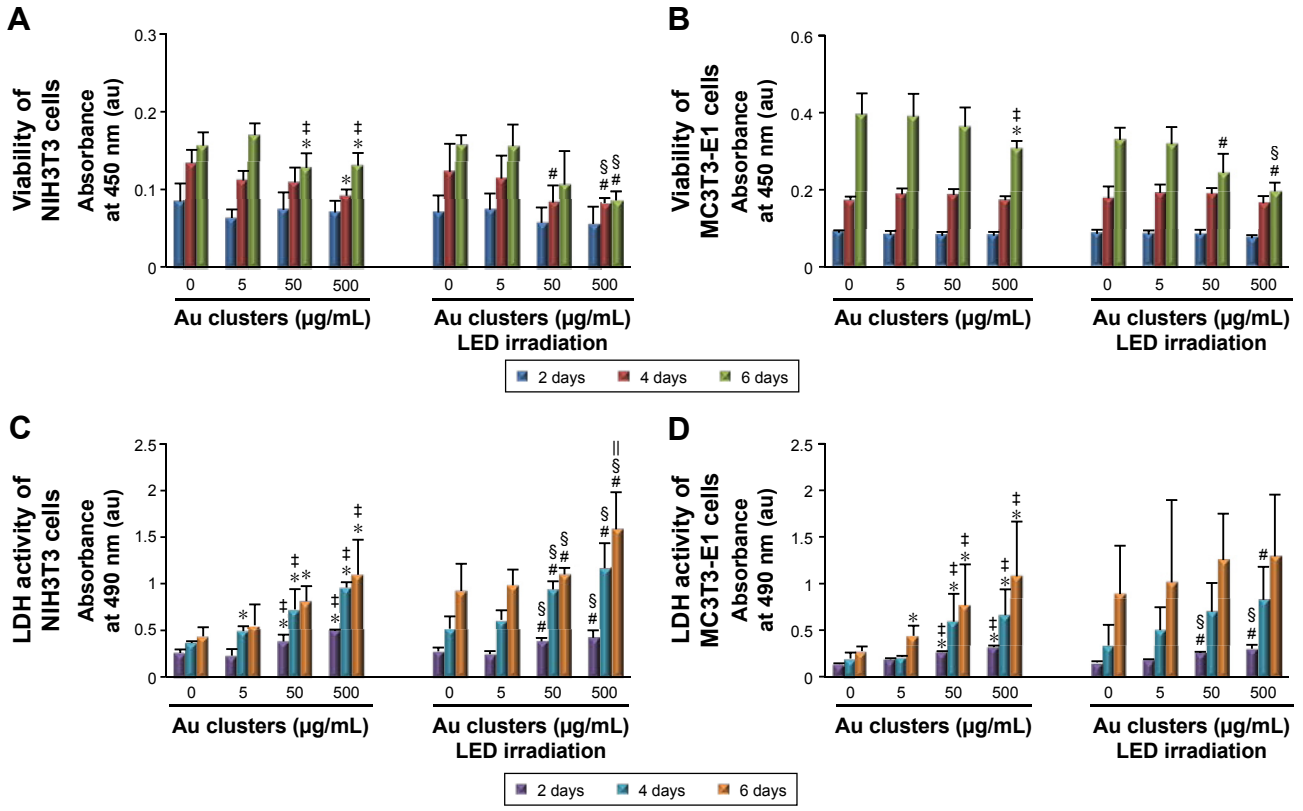

Figure 6 Cytotoxic effects on fibroblastic and osteoblastic cells at 2, 4, and 6 days (n=6, mean ± standard deviation).
Notes: (**A**) Viability of NIH3T3 cells. (**B**) Viability of MC3T3-E1 cells. (**C**) LDH activity of NIH3T3 cells. (**D**) LDH activity of MC3T3-E1 cells: *$P<0.05$ vs 0 μg/mL Au clusters; #$P<0.05$ vs 0 μg/mL Au clusters after LED irradiation; ‡$P<0.05$ vs 5 μg/mL Au clusters; §$P<0.05$ vs 5 μg/mL Au clusters after LED irradiation; ||$P<0.05$ vs 50 μg/mL Au clusters after LED irradiation.
Abbreviations: au, arbitrary unit; LDH, lactate dehydrogenase; LED, light-emitting diode.

and around the destroyed *S. mutans* cells, suggesting that its substance was Au cluster aggregate. In addition, fluorescence examination revealed that $Au_{25}(Capt)_{18}$ clusters in culture medium agglutinated around *S. mutans* (Figure 3I). Accordingly, we speculate that Au clusters attach to bacterial cells and persistently provide $^1O_2$ to *S. mutans*, thus exerting an antimicrobial effect. The lactic acid production of *S. mutans* was also inhibited by photoexcited Au clusters, similar to bacterial growth. The reduction of lactic acid production may have been associated with inhibition of *S. mutans* growth. Conversely, previous reports revealed that the metabolic function of bacterial cells was downregulated by $^1O_2$ through oxidation of amino acids and DNA damage.[31] Therefore, application of $Au_{25}(Capt)_{18}$ clusters under blue LED light would be beneficial for aPDT against *S. mutans*.

The combined application of $Au_{25}(Capt)_{18}$ clusters and light irradiation strongly diminished the turbidity of periodontal bacterial suspensions, *A. actinomycetemcomitans* and *P. gingivalis*, suggesting that photoexcited Au clusters consistently exhibited an antibacterial effect on periodontal bacteria. According to the report of Bhatti et al,[32] $^1O_2$ showed sufficient effectiveness on Gram-negative bacteria including *A. actinomycetemcomitans* and *P. gingivalis* as well as Gram-positive bacteria, such as *S. mutans*. Even at a low concentration (5 μg/mL), application of Au clusters was effective against *A. actinomycetemcomitans* and *P. gingivalis*. In addition, the no irradiation group showed reduced turbidity of periodontal bacterial suspensions. Since the culture medium including $Au_{25}(Capt)_{18}$ clusters was exposed to visible light in this study, a small amount of $^1O_2$ may have been generated, which affected bacterial growth. We also speculate that Gram-negative bacteria may be more sensitive to the antimicrobial effect of $Au_{25}(Capt)_{18}$ clusters; however, further research is needed to elucidate the precise mechanisms.

To confirm the biocompatibility of $Au_{25}(Capt)_{18}$ clusters, we carried out the cytotoxic test in two cell lines associated with periodontal tissue.[33,34] SEM images and LIVE/DEAD staining after 24 h of culture showed that fibroblastic and osteoblastic cells receiving photoexcited $Au_{25}(Capt)_{18}$ clusters normally spread on the culture dish and fluoresced as live cells. In addition, expression of f-actin and vinculin,

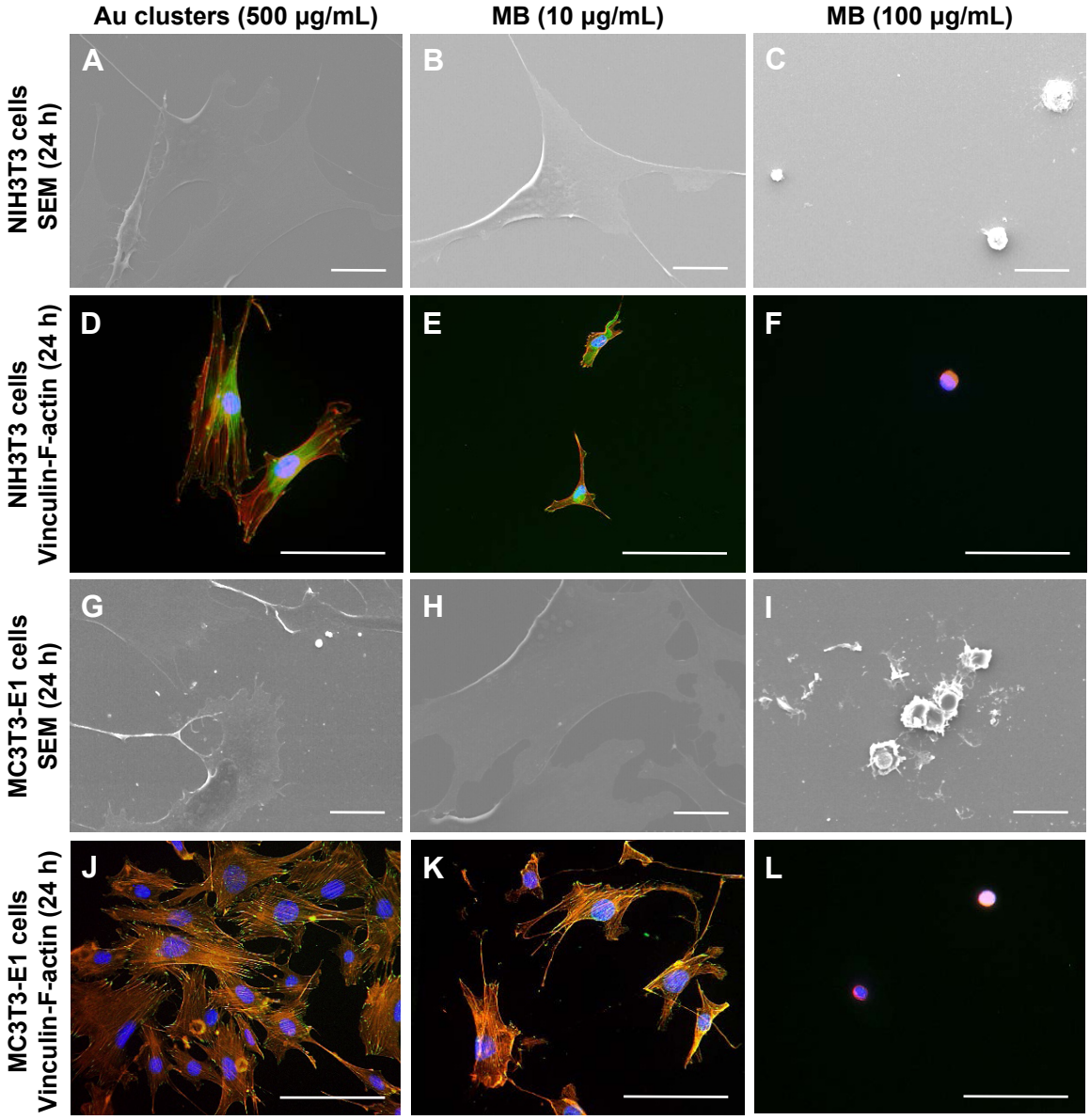

Figure 7 Comparative evaluation of cytotoxicity of $Au_{25}(Capt)_{18}$ clusters and MB after 24-h incubation.
Notes: (**A**–**C**) SEM micrographs of NIH3T3 cells. (**D**–**F**) Vinculin/F-actin double staining of NIH3T3 cells. (**G**–**I**) SEM micrographs of MC3T3-E1 cells. (**J**–**L**) Vinculin-F-actin double staining of MC3T3-E1 cells. Scale bar represents 20 μm (**A**–**C**, **G**–**I**) and 50 μm (**D**–**F**, **J**–**L**).
Abbreviations: MB, methylene blue; SEM, scanning electron microscopy.

associated with cell adhesion, was demonstrated similar to control, suggesting that the cytocompatibility of $Au_{25}(Capt)_{18}$ clusters was good. Normally, strong antibacterial activity frequently leads to strong cytotoxicity; therefore, cytocompatibility of $Au_{25}(Capt)_{18}$ clusters would be advantageous for biomedical application. However, application of $Au_{25}(Capt)_{18}$ clusters dose-dependently decreased cell viability and increased LDH production after 4-day incubation, in particular, under conditions receiving light irradiation. It is considered that long-term application of $Au_{25}(Capt)_{18}$ clusters would gradually exert cytotoxicity by $^1O_2$ generation. Therefore, we believe that short-term application of $Au_{25}(Capt)_{18}$ clusters would be necessary for aPDT to weaken potential cytotoxicity. Since photoexcited $Au_{25}(Capt)_{18}$ clusters at a concentration of 5 μg/mL well suppressed the growth of periodontal bacteria and rarely inhibited growth of fibroblastic and osteoblastic cells after 2-day incubation, we speculate that 5 μg/mL Au clusters would be safe for periodontal aPDT. However, in vivo dynamics should be assessed to determine the optimal application dose of Au clusters against periodontal disease.

We also evaluated the biocompatible properties of 500 μg/mL $Au_{25}(Capt)_{18}$ clusters compared with 10 and 100 μg/mL MB, which are used in conventional aPDT

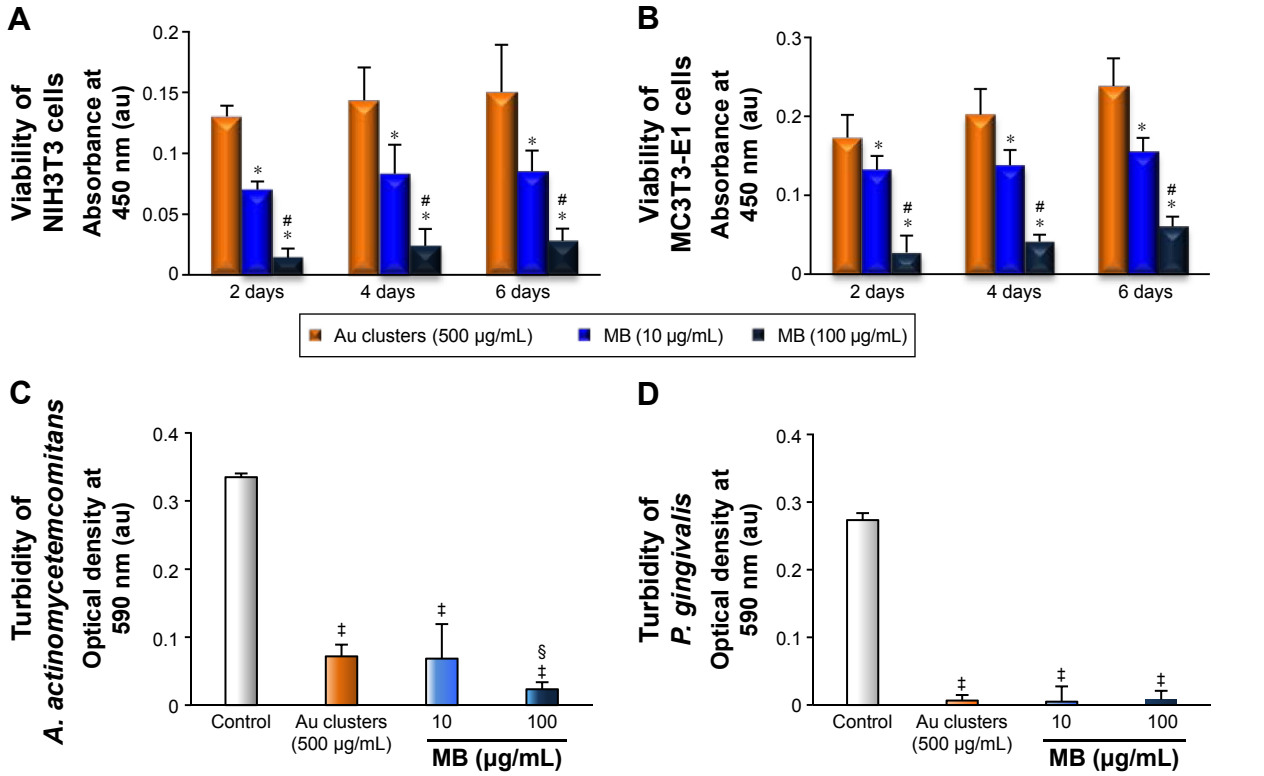

Figure 8 Cytotoxic and antimicrobial effects of $Au_{25}(Capt)_{18}$ clusters and MB.

Notes: (**A**, **B**) Viability of NIH3T3 cells (**A**) and MC3T3-E1 cells (**B**) at 2, 4, and 6 days (n=5, mean ± SD). *$P<0.05$ vs 500 μg/mL Au clusters; #$P<0.05$ vs 10 μg/mL MB. (**C**, **D**) Turbidity assays of *A. actinomycetemcomitans* (**C**) and *P. gingivalis* (**D**) after 24-h incubation (n=5, mean ± SD). ‡$P<0.05$ vs control; §$P<0.05$ vs 500 μg/mL Au clusters and 10 μg/mL MB.

Abbreviations: au, arbitrary unit; MB, methylene blue; SD, standard deviation; *A. actinomycetemcomitans*, *Aggregatibacter actinomycetemcomitans*; *P. gingivalis*, *Porphyromona gingivalis*.

procedures. *A. actinomycetemcomitans* and *P. gingivalis* turbidity receiving 500 μg/mL $Au_{25}(Capt)_{18}$ clusters was equivalent to those receiving 10 μg/mL MB, regardless of light irradiation. However, the viability of fibroblastic and osteoblastic cells was remarkably suppressed by application of MB compared to Au clusters. Furthermore, immunostaining examination indicated that MB caused poor cell spreading and vinculin expression compared with $Au_{25}(Capt)_{18}$ clusters, in particular, 100 μg/mL MB resulted in strong cellular dysfunction. Thus, MB and its complex might decrease cell adhesion and proliferation when mobilized in aPDT. As the effect of light irradiation was not evaluated, the direct interaction between organic substances and bacteria might play a major role in cytotoxic effects.

LED irradiation alone slightly increased the antimicrobial effect and LDH activity in this study. Chui et al[20] reported that blue LED greatly suppressed gene expression associated with DNA replication and bacterial cell division compared to red LED, resulting in inhibition of *P. gingivalis*. Therefore, the blue light source in aPDT might provide a favorable auxiliary for antimicrobial effects. Since $Au_{25}(Capt)_{18}$ clusters possess strong absorbance in the wavelength region of blue LED light, the antimicrobial effect of $Au_{25}(Capt)_{18}$ clusters may be promoted by the coupling effect of blue LED light-induced production of $^1O_2$ and the action of blue light. Further studies are necessary to assess the potential synergistic antimicrobial effect between $Au_{25}(Capt)_{18}$ clusters and optical devices.

Conclusion

The antimicrobial and cytocompatible effects of $Au_{25}(Capt)_{18}$ clusters under blue LED light irradiation were examined in vitro. Fluorescence measurement revealed that $^1O_2$ was generated when $Au_{25}(Capt)_{18}$ clusters were irradiated with blue LED light. Application of photoexcited $Au_{25}(Capt)_{18}$ clusters significantly inhibited the growth of oral bacterial cells, including *S. mutans, A. actinomycetemcomitans*, and *P. gingivalis*. In addition, $Au_{25}(Capt)_{18}$ clusters under blue LED rarely exhibited cytotoxicity in fibroblastic NIH3T3 and osteoblastic MC3T3E1 cells, in particular, at low doses. In comparison with a typical organic dye photosensitizer, MB, $Au_{25}(Capt)_{18}$ clusters were biosafe. Therefore, $Au_{25}(Capt)_{18}$ clusters and blue LED are expected to be beneficial for aPDT related to dental therapy.

Acknowledgments

The authors acknowledge Dr Saori Tanaka and Ms Kanako Shitomi from the Department of Periodontology and Endodontology, and Dr Tadashi Iizuka from the Support Section for Education and Research, Hokkaido University Graduate School of Dental Medicine, for their technical support in the cytocompatible assessments. The authors also acknowledge Prof Kenichiro Shibata and Dr Ayumi Saeki from the Department of Oral Pathobiological Science, Hokkaido University Graduate School of Dental Medicine, for their educational support in the assessments of antibacterial effects. This work was supported by JSPS KAKENHI (Grant Nos JP15H03520, JP15H03526, JP26505011, JP26107719, and JP16K11822) and Hitachi Metals Materials Science Foundation. A part of this work was supported by the Nanotechnology Platform Program (Molecule and Material Synthesis) of the Ministry of Education, Culture, Sports, Science and Technology (MEXT), Japan.

Disclosure

The authors report no conflicts of interest in this work.

References

1. Konopka K, Goslinski T. Photodynamis therapy in dentistry. *J Dent Res*. 2007;86(8):694–707.
2. Hamblin MR, Hasan T. Photodynamic therapy: a new antimicrobial approach to infectious disease? *Photochem Photobiol Sci*. 2004;3(5):436–450.
3. Henderson BW, Dougherty TJ. How does photodynamic therapy work? *Photochem Photobiol*. 1992;55(1):145–157.
4. El-Hussein A, Harith M, Abrahamse H. Assessment of DNA damage after photodynamic therapy using a metallophthalocyanine photosensitizer. *Int J Photoenergy*. 2012;2012(2):1–10.
5. Plaetzer K, Krammer B, Berlanda J, Berr F, Kiesslich T. Photophysics and photochemistry of photodynamic therapy: fundamental aspects. *Lasers Med Sci*. 2009;24(2):259–268.
6. Wilson M. Lethal photosensitization of oral bacteria and its potential application in the photodynamic therapy of oral infections. *Photochem Photobiol Sci*. 2004;3(5):412–418.
7. Meisel P, Kocher T. Photodynamic therapy for periodontal diseases: state of the art. *J Photochem Photobiol B*. 2005;79(2):159–170.
8. Biel MA. Photodynamic therapy of bacterial and fungal biofilm infections. *Methods Mol Biol*. 2010;635:175–194.
9. Zanin IC, Gonçalves RB, Junior AB, Hope CK, Pratten J. Susceptibility of *Streptococcus mutans* biofilms to photodynamic therapy: an in vitro study. *J Antimicrob Chemother*. 2005;56(2):324–330.
10. Wood S, Metcalf D, Devine D, Robinson C. Erythrosine is a potential photosensitizer for the photodynamic therapy of oral plaque biofilms. *J Antimicrob Chemother*. 2006;57(4):680–684.
11. Rajesh S, Koshi E, Philip K, Mohan A. Antimicrobial photodynamic therapy: an overview. *J Indian Soc Periodontol*. 2011;15(4):323–327.
12. Prasanth CS, Karunakaran SC, Paul AK, et al. Antimicrobial photodynamic efficiency of novel cationic porphyrins towards periodontal Gram-positive and Gram-negative pathogenic bacteria. *Photochem Photobiol*. 2014;90(3):628–640.
13. Soria-Lozano P, Gilaberte Y, Paz-Cristobal MP, et al. In vitro effect photodynamic therapy with differents photosensitizers on cariogenic microorganisms. *BMC Microbiol*. 2015;15(1):187.
14. Parker S. The use of diffuse laser photonic energy and indocyanine green photosensitiser as an adjunct to periodontal therapy. *Br Dent J*. 2013;215(4):167–171.
15. Rosa LP, da Silva FC, Nader SA, Meira GA, Viana MS. Antimicrobial photodynamic inactivation of *Staphylococcus aureus* biofilms in bone specimens using methylene blue, toluidine blue ortho and malachite green: an in vitro study. *Arch Oral Biol*. 2015;60(5):675–680.
16. Christodoulides N, Nikodakis D, Chondros P, et al. Photodynamic therapy as an adjunct to non-surgical periodontal treatment: a randomized, controlled clinical trial. *J Periodontal*. 2008;79(9):1638–1644.
17. Moan J, Berg K. The photodegradation of porphyrins in cells that can be used to estimate the lifetime of singlet oxygen. *Photochem Photobiol*. 1991;53(4):549–553.
18. Crooks J. Haemolytic jaundice in a neonate after intra-amniotic injection of methylene blue. *Arch Dis Child*. 1982;57(11):872–873.
19. Kawasaki H, Kumar S, Li G, et al. Generation of singlet oxygen by photoexcited $Au_{25}(SR)_{18}$ clusters. *Chem Mater*. 2014;26(9):2777–2778.
20. Chui C, Hiratsuka K, Aoki A, Takeuchi Y, Abiko Y, Izumi Y. Blue LED inhibits the growth of *Porphyromonas gingivalis* by suppressing the expression of genes associated with DNA replication and cell division. *Lasers Surg Med*. 2012;44(10):856–864.
21. Kumar S, Jin R. Water-soluble $Au_{25}(Capt)_{18}$ nanoclusters: synthesis, thermal stability, and optical properties. *Nanoscale*. 2012;4(14):4222–4227.
22. Hirakawa K. Fluorometry of singlet oxygen generated via a photosensitized reaction using folic acid and methotrexate. *Anal Bioanal Chem*. 2009;393(3):999–1005.
23. Javed F, Romanos GE. Does photodynamic therapy enhance standard antibacterial therapy in dentistry? *Photomed Laser Surg*. 2013;31(11):512–518.
24. Almeida JM, Theodoro LH, Bosco AF, Nagata MJ, Oshiiwa M, Garcia VG. In vivo effect of photodynamic therapy on periodontal bone loss in dental furcations. *J Periodontal*. 2008;79(6):1081–1088.
25. Lemke RA, Peterson AC, Ziegelhoffer EC, et al. Synthesis and scavenging role of furan fatty acids. *Proc Natl Acad Sci U S A*. 2014;111(33):E3450–E3457.
26. Humphries KM, Szweda LI. Selective inactivation of alpha-ketoglutarate dehydrogenase and pyruvate dehydrogenase: reaction of lipoic acid with 4-hydroxy-2-nonenal. *Biochemistry*. 1998;37(45):15835–15841.
27. Wang Y, Jett SD, Crum J, Schanze KS, Chi EY, Whitten DG. Understanding the dark and light-enhanced bactericidal action of cationic conjugated polyelectrolytes and oligomers. *Langmuir*. 2013;29(2):781–792.
28. Ichinose-Tsuno A, Aoki A, Takeuchi Y, et al. Antimicrobial photodynamic therapy suppresses dental plaque formation in healthy adults: a randomized controlled clinical trial. *BMC Oral Health*. 2014;14:152.
29. Fontana CR, Abernethy AD, Som S, et al. The antibacterial effect of photodynamic therapy in dental plaque-derived biofilms. *J Periodontal Res*. 2009;44(6):751–759.
30. O'Neill JF, Hope CK, Wilson M. Oral bacteria in multi-species biofilms can be killed by red light in the presence of toluidine blue. *Lasers Surg Med*. 2002;31(2):86–90.
31. Cabiscol E, Tamarit J, Ros J. Oxidative stress in bacteria and protein damage by reactive oxygen species. *Int Microbiol*. 2000;3(1):3–8.
32. Bhatti M, MacRobert A, Meghji S, Henderson B, Wilson M. A study of the uptake of toluidine blue O by *Porphyromonas gingivalis* and the mechanism of lethal photosensitization. *Photochem Photobiol*. 1998;68(3):370–376.
33. Pivodova V, Frankova J, Ulrichova J. Osteoblast and gingival fibroblast markers in dental implant studies. *Biomed Pap Med Fac Univ Palacky Olomouc Czech Repub*. 2011;155(2):109–116.
34. Lekic P, McCulloch CA. Periodontal ligament cell populations: the central role of fibroblasts in creating a unique tissue. *Anat Rec*. 1996;245(2):327–341.

Supplementary material

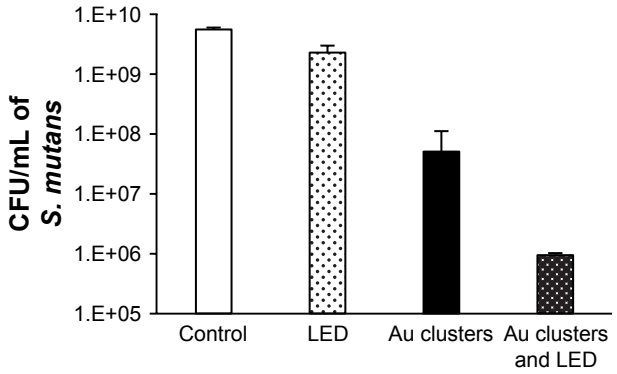

Figure S1 Antimicrobial effects of Au clusters on *S. mutans* after 24-h incubation.
Notes: Number of CFU/mL of *S. mutans*, n=2. Data are expressed as mean ± standard deviation.
Abbreviations: CFU, colony-forming unit; LED, light-emitting diode; *S. mutans*, *Streptococcus mutans*.